

### Isovector and isoscalar spin-flip excitations in even-even $s$ - $d$ shell nuclei excited by inelastic proton scattering

G. M. Crawley,<sup>(a)</sup> C. Djalali,<sup>(a),(b)</sup> N. Marty,<sup>(b)</sup> M. Morlet,<sup>(b)</sup> A. Willis,<sup>(b)</sup> N. Anantaraman,<sup>(a)</sup>  
B. A. Brown,<sup>(a)</sup> and A. Galonsky<sup>(a)</sup>

<sup>(a)</sup>National Superconducting Cyclotron Laboratory and Department of Physics and Astronomy,  
Michigan State University, East Lansing, Michigan 48824

<sup>(b)</sup>Institut de Physique Nucléaire, Orsay 91406, France

(Received 14 July 1988)

Forward-angle cross sections for  $1^+$  states have been measured in  $^{24,26}\text{Mg}$ ,  $^{28}\text{Si}$ , and  $^{32}\text{S}$  by 201 MeV proton inelastic scattering. Comparisons are made with  $(\gamma, \gamma')$ ,  $(e, e')$ , and  $(p, n)$  results. The measured strength is compared with microscopic distorted-wave Born approximation calculations using large-scale shell-model wave functions. Ratios of experimental to theoretical  $1^+$  strengths are given. Almost no quenching is observed.

#### I. INTRODUCTION

The study of spin excitations is important because it provides information about the basic spin dependence of the nuclear force. Much of the recent interest in spin excitation stems from the discrepancy between the predicted and observed strength in Gamow-Teller transitions studied in  $(p, n)$  reactions,<sup>1</sup> in  $M1$  transitions induced by electromagnetic probes,<sup>2,5</sup> and in the spin-flip excitation of  $1^+$  states in  $(p, p')$  reactions.<sup>4</sup> Generally, more strength is predicted than is observed experimentally, up to a factor of 3 in some cases, and therefore the discrepancy is referred to as quenching. Various mechanisms have been proposed to explain this quenching including the admixture with high-lying many-particle-many-hole configurations via the tensor force or virtual  $(\Delta-h)$  excitations. The latter mechanism can only apply to  $1^+$ ,  $\Delta T=1$  states because of the quantum numbers of the  $\Delta$  resonance ( $J=\frac{3}{2}$ ,  $T=\frac{3}{2}$ ).

The present experiment attempts to cast further light on this problem by studying both  $1^+$ ,  $T=0$  and  $1^+$ ,  $T=1$  states excited by the  $(p, p')$  reaction at 201 MeV to see whether the quenching is reduced for the isoscalar ( $T=0$ ) states, as would be expected if the  $\Delta-h$  admixture was the dominant quenching mechanism. Such studies can only be made using the  $(p, p')$  reaction since isoscalar states are strongly suppressed in electromagnetic transitions. The region of nuclei chosen for study was the  $s$ - $d$  shell because there are a number of even-even nuclei in this region with  $T=0$  ground states. Therefore, both  $T=0$  and  $T=1, 1^+$  states should exist in these nuclei, and these states are excited by isoscalar and isovector transition operators, respectively.

In addition, the region between  $^{12}\text{C}$  and  $^{48}\text{Ca}$  is particu-

larly appropriate to study quenching. The ratio of experimental to predicted strength varies from approximately unity for the 15.1 MeV  $1^+$  state in  $^{12}\text{C}$  (no quenching) to about 0.4 in  $^{48}\text{Ca}$ . It would be interesting to observe the variation of the quenching for other even-even nuclei between these two nuclei. Nuclear resonance fluorescence experiments<sup>3</sup> have shown that for nuclei of the  $s$ - $d$  shell, the ratio of experimental to predicted  $1^+$  strength is of the order of 0.9–1, but these experiments are limited by the particle emission threshold.

Excellent shell-model wave functions for  $1^+$  states are available for the  $s$ - $d$  shell nuclei;<sup>5,6</sup> they predict noticeable orbital contributions to the electromagnetic excitation of some states. Isospin mixing is also predicted for some  $1^+$  states in  $^{24}\text{Mg}$ .<sup>7</sup> All these predictions can be tested by comparing  $(p, p')$  with  $(e, e')$  data. We have therefore carried out  $(p, p')$  scattering on  $^{18}\text{O}$ ,  $^{20}\text{Ne}$ ,  $^{22}\text{Ne}$ ,  $^{24}\text{Mg}$ ,  $^{26}\text{Mg}$ ,  $^{28}\text{Si}$ , and  $^{32}\text{S}$ . The results on the oxygen<sup>8</sup> and the neon isotopes<sup>9</sup> have already been published. Preliminary results of the  $^{28}\text{Si}$  measurements have also been reported previously<sup>10</sup> and only an update will be presented here. The experimental procedures, including the target production and the determination of the absolute cross sections, will be described in Sec. II. An outline of the shell-model wave functions and the reaction calculations will be given in Sec. III. Results and discussion are presented in Sec. IV and a summary and conclusions are given in Sec. V.

#### II. EXPERIMENTAL PROCEDURE

The measurements were carried out using a 201 MeV proton beam from the Orsay synchrocyclotron. The general experimental arrangement used to obtain proton

spectra at angles as small as  $2^\circ$  with very low background has been described previously.<sup>11</sup> The Mg targets used were self-supporting metallic foils. The  $^{24}\text{Mg}$  target had a thickness of  $15.4 \text{ mg/cm}^2$ , and the  $^{26}\text{Mg}$  target a thickness of  $5.3 \text{ mg/cm}^2$ . The Si target used in the first stage of the experiment was etched from a piece of natural silicon and had a thickness of about  $6.1 \text{ mg/cm}^2$ . Later a more uniform, though thicker ( $17.7 \text{ mg/cm}^2$ ), target was employed.

In the case of  $^{32}\text{S}$ , two targets were used. A thin target was prepared by pouring molten sulfur vapor onto cold water where the vapor condensed as an elastic film. This film was picked up on a wire loop and stretched over a target frame. Up to two or three layers were used to produce a target of about  $7 \text{ mg/cm}^2$ . This target was used to obtain good resolution data. For absolute normalization purposes, a thicker target was used. This target was prepared by pressing sulfur powder under a pressure of  $30\,000 \text{ kg/cm}^2$ . This produced a brittle flake with uniformity of about 5% and a total thickness of  $20 \text{ mg/cm}^2$ . The uniformity was measured after the target had been used by dividing it into pieces and weighing the pieces.

A check on the absolute normalization was carried out using the 200 MeV proton beam at the TRIUMF accelerator. Measurements on  $^{24}\text{Mg}$ ,  $^{28}\text{Si}$ , and  $^{32}\text{S}$  were made with a number of targets of various thicknesses. Absolute cross sections were also remeasured on the same three nuclei at Orsay. These measurements from TRIUMF and Orsay agreed in all cases to within a few percent. The uncertainties on the absolute cross sections are of order  $\pm 5\%$  for  $^{24,26}\text{Mg}$  and  $^{28}\text{Si}$ , and  $\pm 10\%$  for  $^{32}\text{S}$ .

The overall resolution obtained at Orsay varied from about 60 keV for the metallic foils to between 80 and 90 keV for the  $^{32}\text{S}$ .

### III. THEORETICAL MODELS

#### A. Shell-model wave functions and matrix elements

Most low-lying levels in the  $8 \leq (N, Z) \leq 20$  region can be described in terms of an  $s$ - $d$  shell model, in which eight neutrons and eight protons are confined to the filled  $0s$  and  $0p$  orbits and the remaining, active, nucleons occupy the  $1s$  and  $0d$  orbits, of  $n, l, j$  values  $1s_{1/2}$ ,  $0d_{5/2}$ , and  $0d_{3/2}$ . Recent calculations within this  $s$ - $d$  model space have produced wave functions from a unified formulation of the model Hamiltonian which have been quite successful in reproducing binding energies and excitation energies.<sup>12</sup> These wave functions span the complete spaces of  $0d_{5/2}$ ,  $1s_{1/2}$ , and  $0d_{3/2}$  configurations, which is a critical aspect when considering matrix elements of operators, such as the spin operator, for which the transitions between the spin-orbit partners are of paramount importance.<sup>13</sup>

The  $s$ - $d$  shell Hamiltonian<sup>12</sup> is assumed to consist of one- and two-body isospin-conserving interactions and, more specifically, has a fixed one-body spectrum and a single set of two-body matrix elements. These two-body matrix elements are scaled for application to a given  $A$  value by the factor  $(18/A)^{1/3}$ . Hamiltonian matrices are diagonalized to produce a family of wave functions

$|NTJn\rangle$ , where  $N = A - 16$ ,  $T$  and  $J$  designate the total isobaric and angular-momentum spin values, and  $n$  is the counting index which identifies a particular eigenstate of the  $NTJ$  set. The Hamiltonian parameters (the single-particle energies and two-body matrix elements) were obtained from a least-squares fit to 447  $s$ - $d$  shell binding energy and excitation energy data.<sup>12</sup>

The reduced matrix element between multiparticle shell-model wave functions of any one-body operator  $O^{\Delta J, \Delta T}$ , of tensor rank  $\Delta J$  in angular momentum space and tensor rank  $\Delta T$  in isospin space, can be expressed as a sum of the products of the elements of the multiparticle transition amplitudes multiplied by single-particle matrix elements. For the  $s$ - $d$  shell-model space there are ten independent single-particle matrix elements for  $\Delta J = 1$ , corresponding to the  $j$ - $j'$  combinations  $0d_{5/2}$ - $0d_{5/2}$ ,  $0d_{5/2}$ - $0d_{3/2}$ ,  $1s_{1/2}$ - $1s_{1/2}$ ,  $1s_{1/2}$ - $0d_{3/2}$ , and  $0d_{3/2}$ - $0d_{3/2}$  for the  $\Delta T = 0$  (isoscalar) and  $\Delta T = 1$  (isovector) couplings. (The  $j$ - $j'$  and  $j'$ - $j$  terms can be combined for each pair of inequivalent orbits.) The corresponding multiparticle transition amplitudes are uniquely and completely determined by the specification of the model Hamiltonian and embody its entire predictive contents for rank-one operators.

With these wave functions it has been possible to analyze systematically experimental  $M1$  and Gamow-Teller data from the  $s$ - $d$  shell with a minimum of concern for the effects of varying space truncations and Hamiltonian formulations which vitiate most quantitative shell-model analyses of heavier nuclei. More details about these calculations are given in Ref. 5.

Calculations allowing isospin mixing<sup>7</sup> have also been performed. Noticeable mixing of  $\Delta T = 0$  and  $1, 1^+$  strength is predicted in  $^{24}\text{Mg}$ .

#### B. Distorted-wave calculations

Microscopic distorted-wave Born-approximation (DWBA) calculations of  $(p, p')$  cross sections for  $1^+$  states have been performed using the code DW81 (Ref. 14) which is a modified and extended version of the code DWBA70.<sup>15</sup> The one-body transition densities were obtained from the wave functions described above without any normalization parameter. The effective nucleon-nucleon interaction used in the calculations is the one derived by Franey and Love<sup>16</sup> from 210 MeV free nucleon-nucleon interaction. The optical potential used were obtained by extrapolating the parameterization of Schwandt *et al.*<sup>17</sup> to 200 MeV. For  $^{28}\text{Si}$  and  $^{24}\text{Mg}$ , optical-potential parameters obtained at TRIUMF at 200 and 250 MeV (Refs. 18 and 19) were also used. The results obtained with both sets of optical-potential parameters agree to within 5% at forward angles ( $\theta \leq 15^\circ$ ).

Distorted-wave impulse approximation (DWIA) calculations for  $(p, p')$  cross sections have also been performed with the code RESEDA (Ref. 20) using the nucleon-nucleon phase shifts given by the Paris potential.<sup>21</sup> These calculations are in agreement with those of DW81.

For natural parity states like  $0^+$ ,  $1^-$ ,  $2^+$ ,  $3^-$ , ... macroscopic DWBA calculations were performed with the code DWUCK (Ref. 22) using standard collective transi-

tion potentials.<sup>23</sup> For each nucleus, the ratio ( $R$ ) of the experimental to the predicted cross sections for the total  $1^+$  strength will be given.

### C. Comparison between $(p,p')$ and $(e,e')$ results

Assuming the impulse approximation, it has been shown previously<sup>8,24</sup> that for a  $1^+$  excitation the  $(p,p')$  cross section at small momentum transfer ( $\theta \approx 0^\circ$ ) is proportional to a distortion factor, the square of the modulus of the nucleon-nucleon interaction responsible for the transition, and the square of a reduced matrix element which is directly related to the spin component  $B(\sigma)$  of the transition probability  $B(M1)$ . The  $B(\sigma)$  value is obtained by setting  $g_l=0$  and  $g_s$  equal to the free-nucleon value in the  $B(M1)$  expression. Using the shape of the calculated angular distribution, one can extrapolate the measured  $(p,p')$  cross section to  $\theta=0^\circ$ . To obtain the  $B(\sigma)$  value, one also needs to know the modulus of the interaction involved in the transition. This is the case only for pure transitions in  $N=Z$  nuclei (i.e., pure  $T=1$  or pure  $T=0, 1^+$  states). For nuclei like  $^{26}\text{Mg}$  with  $N$  not equal to  $Z$ , the interaction responsible for the  $1^+$  transitions is a mixture of isoscalar and isovector spin-dependent terms of the nucleon-nucleon interaction. The relative weight of the different terms varies from state to state. In this case, we have proceeded in the following way: For each predicted state we have calculated the ratio of the theoretical  $B(\sigma)$  value to the theoretical cross section at zero degrees; the average value of this ratio was applied to the experimental cross sections in order to deduce the  $B(\sigma)$  values. Uncertainties as large as 20% resulted from this procedure. By comparing these extracted  $B(\sigma)$  values to the  $B(M1)$  values measured in  $(e,e')$  or  $(\gamma,\gamma')$  reactions, the importance of the orbital term in the electromagnetic excitation could be deduced.

## IV. EXPERIMENTAL RESULTS AND DISCUSSION

### A. $^{24}\text{Mg}$

A spectrum from  $^{24}\text{Mg}$   $(p,p')$  at a laboratory angle of  $3^\circ$  is shown in Fig. 1. At this forward angle, as has been observed previously in other nuclei, the spectrum is dominated by angular-momentum transfer  $l=0$  transitions. Only about twenty significant states are seen above a smooth background up to an excitation energy of 17 MeV, even though the level density in the region between 6 and 17 MeV is very high.<sup>25</sup>

Angular distributions for some representative states of different  $J^\pi$  are shown in Fig. 2. The angular distributions of some  $1^+$  states are given in Fig. 3. The solid lines in Fig. 2 are macroscopic DWBA calculations described in Sec. III B. Clearly, these angular distributions do allow a rather unambiguous identification of the  $l$  transfer. For example, the angular distribution for the  $2^+$  state at 7.35 MeV has a minimum near  $4^\circ$  and rises to a peak near  $12^\circ$ . States with  $l$  transfer greater than  $l=2$  show similar behavior but peak at even larger angles. For example, the known  $3^-$  state at 7.62 MeV excitation energy has a minimum near  $5^\circ$  and peaks beyond  $12^\circ$ .

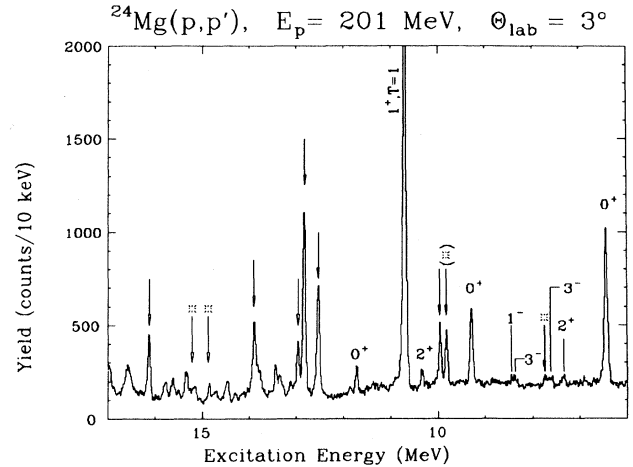


FIG. 1. Inelastic  $(p,p')$  spectrum measured at  $3^\circ$  on  $^{24}\text{Mg}$ .  $1^+$  states are indicated by arrows.

The known  $1^-$  state at 8.44 MeV has a rather flat angular distribution out to  $10^\circ$ , which seems characteristic of an  $l=1$  transfer.

The  $l=0$  transfers show a forward peaked angular distribution. Among the  $l=0$  transitions, it appears to be possible to distinguish  $0^+$  states from  $1^+$  states. With less certainty, even  $T=0, 1^+$  states can also be distinguished from  $T=1, 1^+$  states. The cross sections of  $0^+$  states decrease even more rapidly with angles than those of  $1^+, T=1$  states, and the angular distributions have a minimum near  $8^\circ$ . The known  $0^+$  states at 6.43 and 11.74 MeV provide good examples; the angular distribution for the 6.43 MeV state is shown in Fig. 2. Similar behavior of  $0^+$  angular distributions was observed in studies of the oxygen isotopes.<sup>8</sup> As shown in Fig. 2, there is a state observed at 9.30 MeV excitation energy which has a characteristic  $0^+$  angular distribution. While there

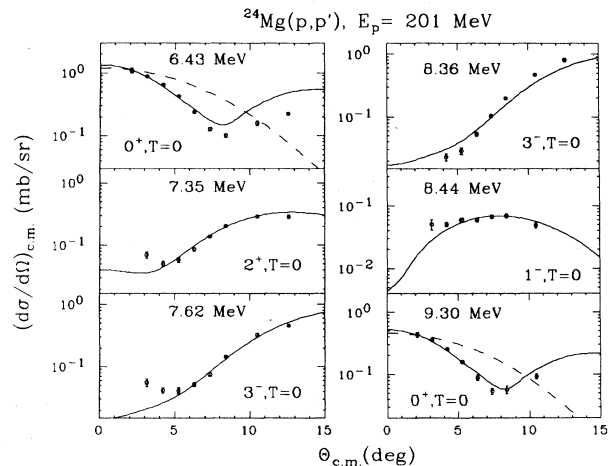


FIG. 2. Measured  $(p,p')$  angular distributions for some natural parity states in  $^{24}\text{Mg}$  compared with normalized macroscopic DWBA calculations. For  $0^+$  states, the predicted  $1^+$  angular distribution is given as a dashed curve for comparison.

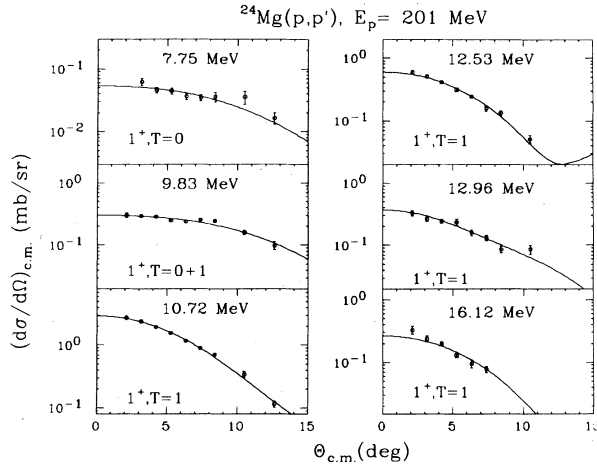


FIG. 3. Measured  $(p,p')$  angular distributions for some  $1^+$  states in  $^{24}\text{Mg}$  compared in shape with microscopic DWIA calculations.

are three known states close to this energy,<sup>25</sup> none have  $J^\pi=0^+$ . We conclude that there is an additional state at 9.30 MeV with  $J^\pi=0^+$  which is excited about half as strongly as the  $0^+$  state at 6.43 MeV.

There is also an indication of systematic differences between the angular distributions for  $1^+, T=1$  states such as the 10.72 and 12.53 MeV states and for  $1^+, T=0$  states such as the 9.83 MeV state. The angular distributions of the  $T=0$  states are somewhat flatter due to the different momentum-transfer dependence of the isoscalar and isovector pieces of the nucleon-nucleon interaction. This behavior is predicted rather well by the DWIA calculations. A similar result was noted previously<sup>10</sup> in  $^{28}\text{Si}$ . We have used this behavior of the angular distributions to assign the isospin as well as the  $J^\pi$  of a number of states, especially at higher excitation energy. The angular distributions are shown in Fig. 3. Table I gives a list

of all the  $1^+$  states with their isospin assigned in this way.

The angular distributions of the first two known  $1^+, T=0$  states at 7.75 and 9.83 MeV excitation energy are reasonably well described by the DWIA calculations, especially the stronger state at 9.83 MeV. Similarly, the angular distribution of the strong known  $1^+, T=1$  state at 10.72 MeV agrees well with theoretical predictions. In Ref. 25, three  $1^+$  states are listed at 12.525, 12.815, and 12.892 MeV with no isospin specification. The state at 12.53 MeV is well matched by a  $1^+, T=1$  calculation. For the 12.82 MeV state the  $1^+, T=1$  fit is less good, possibly because of an overlap with a higher spin state whose cross section rises beyond  $7^\circ$ . We have made a tentative isospin assignment of  $T=1$  to the 12.82 MeV state. We see no evidence for the state at 12.892 MeV. The two states on either side at 12.82 and 12.96 MeV are seen and are clearly resolved. We can set an upper limit on the cross section for the 12.892 MeV of about  $50 \mu\text{b/sr}$  at a center of mass angle of  $2.2^\circ$ . The known state at 12.96 MeV is listed as a  $J=1, T=0$  state of unknown parity in Ref. 25. This state has an angular distribution well fitted by the calculation of a  $1^+, T=1$  state predicted at 12.75 MeV.

In addition to these known  $1^+$  states, there are five more states below 17 MeV excitation energy which are good candidates for  $1^+, T=0$  or  $1^+, T=1$  states. Most of these states are rather weak except for the state observed at 16.12 MeV which is quite strong and is well fitted by a  $1^+, T=1$  calculation. At high excitation energy, where the background subtraction is less certain, the angular distributions do not clearly distinguish the  $1^+, T=0$  states from  $1^-$  states. However, since the states in question are quite weak, this uncertainty does not significantly affect the total  $1^+$  strength observed.

The excitation energies, isospins, cross sections at  $3^\circ$  and  $B(\sigma)$  values extracted as described in Sec. III C for all the  $1^+$  states are given in Table I and compared with results from  $(\gamma, \gamma')$  (Ref. 3) and  $(e, e')$  (Ref. 26) reactions. In a  $(p, n)$  experiment<sup>27</sup> very few  $1^+$  states are given and

TABLE I. Excitation energies, isospins, cross sections at  $3^\circ$ , and extracted  $B(\sigma)$  values obtained for  $1^+$  states in  $^{24}\text{Mg}$ . The results obtained in  $(e, e')$  and  $(\gamma, \gamma')$  experiments are given for comparison.

$E_x$ (MeV)	$(p, p')$ <sup>a</sup> $T$	$(d\sigma/d\Omega)_{3^\circ}$ (mb/sr)	$B(\sigma)$ ( $\mu_n^2$ )	$(\gamma, \gamma')$ <sup>b</sup>		$(e, e')$ <sup>c</sup>	
				$E_x$ (MeV)	$B(M1)$ ( $\mu_n^2$ )	$E_x$ (MeV)	$B(M1)$ ( $\mu_n^2$ )
7.75	0	0.06±0.01	0.02±0.01				
9.83	(0,1)	0.30±0.02	0.29±0.02	9.83	0.30±0.11	9.85	0.28±0.07
9.97	1	0.29±0.03	0.38±0.03	9.97	0.86±0.16	9.97	1.17±0.19
10.72	1	2.40±0.10	2.75±0.20	10.71	2.69±0.36	10.70	2.82±0.25
12.53	1	0.51±0.03	0.60±0.03				
12.82	1	0.75±0.03	0.85±0.03				
12.96	1	0.27±0.02	0.37±0.02				
13.90	1	0.40±0.05	0.56±0.09				
14.87	0	0.07±0.01	0.02±0.01				
15.22	0	0.12±0.02	0.03±0.01				
16.12	1	0.24±0.03	0.31±0.06				

<sup>a</sup> Present work.

<sup>b</sup> Reference 3.

<sup>c</sup> Reference 26.

because of the relatively poor energy resolution, a meaningful comparison with the  $(p, p')$  results is not possible.

Unfortunately, there are no new electron scattering results on  $^{24}\text{Mg}$ . The most recent results are summarized in a review article by Fagg.<sup>26</sup> Recent high-quality work by Berg *et al.*<sup>3</sup> used the nuclear resonance fluorescence technique, but of course this method is limited to states which occur below the proton emission threshold at 11.7 MeV excitation energy in  $^{24}\text{Mg}$ . Only three states, located at 9.83, 9.97, and 10.71 MeV, are given in both electromagnetic reactions. The last one is the most strongly excited state in all the experiments, and there is excellent agreement between the  $B(\sigma)$  value extracted from the present work and the  $B(M1)$  values obtained by electromagnetic excitation. This agreement means that the orbital contribution to the electromagnetic excitation of this state is negligible.

Two models are available to describe  $1^+$  states in  $^{24}\text{Mg}$ : model I, with no isospin mixing,<sup>5</sup> and model II, which allows isospin mixing.<sup>7</sup> Both models give the right energy for the strongest peak (10.63 and 10.57 MeV, respectively) and the right  $B(\sigma)$  value (2.55 and 2.49), but both predict an enhancement of 30% of the  $B(M1)$  value due to orbital effects which is not seen experimentally. In Fig. 4, the theoretical  $B(M1)$  and  $B(\sigma)$  strengths given by model I and the experimental  $B(\sigma)$  values for the  $1^+$  states in  $^{24}\text{Mg}$  are shown. No isospin mixing has been assumed to extract the experimental  $B(\sigma)$  values.

For the observed state at 9.97 MeV, the  $B(M1)$  value is at least twice as large as the  $B(\sigma)$  value measured in the present experiment, suggesting an important orbital contribution to the electromagnetic excitation of this state. Both models predict such an interference for a state near 10 MeV.

For the state at 9.83 MeV, the  $B(\sigma)$  and  $B(M1)$  values agree. The  $(p, p')$  angular distribution is flat and characteristic of a  $1^+$ ,  $\Delta T=0$  state. However, the fact that this state is excited in  $(\gamma, \gamma')$  as well as in  $(e, e')$  suggests that it is not a pure  $T=0$  state. Model I predicts a pure  $T=0$

state at 9.98 MeV with a  $B(M1)$  value of  $0.14 \mu_n^2$ . Model II predicts a dominantly  $T=0$  state at 9.92 MeV; due to isospin mixing the predicted  $B(M1)$  value is increased to  $0.66 \mu_n^2$  which is larger than  $(0.28-0.30)\mu_n^2$  measured in the different experiments. The centroid energy for the  $\Delta T=1$  transitions is 11.84 MeV to be compared to the predicted value 11.61 MeV.

In making comparisons between observed and predicted strength, it is more reliable to make comparisons of the total strength observed and predicted rather than to try to make comparisons state by state. Furthermore, due to the prediction by model II of isospin mixing in  $^{24}\text{Mg}$ , it is not justified to separate the isoscalar from the isovector  $1^+$  strength. Therefore, the comparison between theory and experiment is done for the total  $1^+$  strength. The ratio  $R$  of experimental to theoretical cross section for the total  $1^+$  strength is  $1.16 \pm 0.10$  for model I and  $1.13 \pm 0.10$  for model II. The uncertainty due to the nature of some weakly excited states is small compared to the uncertainty in the absolute cross section ( $\pm 5\%$ ).

The ratio  $R$  obtained in the  $(\gamma, \gamma')$  experiment, which is limited by the proton emission threshold at 11.7 MeV, is  $0.90 \pm 0.15$  for model I and  $0.88 \pm 0.14$  for model II. For the same excitation energy range, the  $(p, p')$  ratio would be  $1.17 \pm 0.06$  for model I and  $1.01 \pm 0.05$  for model II.

Recent spin transfer measurements in the  $(p, p')$  reaction at 250 MeV (Ref. 28) limited to 15 MeV excitation energy give an average ratio of experimental to predicted spin-flip strength of  $0.80 \pm 0.10$ . For the same excitation energy range, the present experiment gives an  $R$  value of  $1.06 \pm 0.10$ . The small difference between these two ratios could be explained by the somewhat poorer energy resolution in the 250 MeV measurement and the fact that the experimental  $l=0$  spin-flip strength had to be extracted from the measurement of  $\sigma S_{nn}$  at only two angles.<sup>28</sup>

## B. $^{26}\text{Mg}$

A spectrum measured at a laboratory angle of  $3^\circ$  is shown in Fig. 5. As in  $^{24}\text{Mg}$ , most of the peaks observed have a forward peaked angular distribution characteristic of a  $1^+$  state. The strongest  $1^+$  state in  $^{26}\text{Mg}$  at 10.64 MeV has an excitation energy close to the energy of the dominant state in  $^{24}\text{Mg}$  (10.72 MeV). However, the spin-flip strength is more fragmented than in  $^{24}\text{Mg}$ . Such a fragmentation of the  $1^+$  strength, as neutrons are added, has already been observed in the oxygen isotopes<sup>8</sup> and the neon isotopes.<sup>9</sup>

A level located at 8.21 MeV has an angular distribution with a pronounced minimum at  $6.5^\circ$ , characteristic of a  $0^+$  state. Nineteen states have been assigned a  $1^+$  nature; the differential cross sections for some of them are given in Fig. 6. The angular distributions are characteristic of isovector  $1^+$  states. The slope of the measured angular distributions varies from state to state; this variation is also predicted by the theory (see Fig. 6).

The measured excitation energies, cross sections at  $3^\circ$  and  $B(\sigma)$  values deduced from the  $(p, p')$  cross sections are given in Table II. As explained in Sec. III C, the  $B(\sigma)$  values can be extracted for nonpure  $\Delta T=0$  or 1

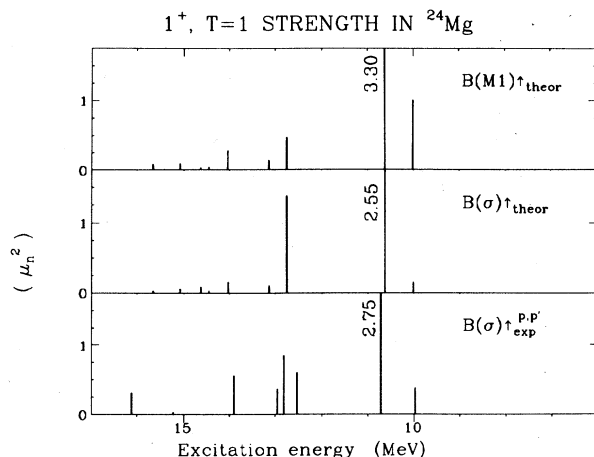


FIG. 4. Predicted spin-flip transition probabilities  $B(\sigma)$  and  $B(M1)$  values for  $1^+$  states in  $^{24}\text{Mg}$  compared with the  $B(\sigma)_{\text{exp}}^{p,p'}$  values extracted from the  $(p, p')$  cross sections. No isospin mixing is assumed. Strengths are given in  $\mu_n^2$ .

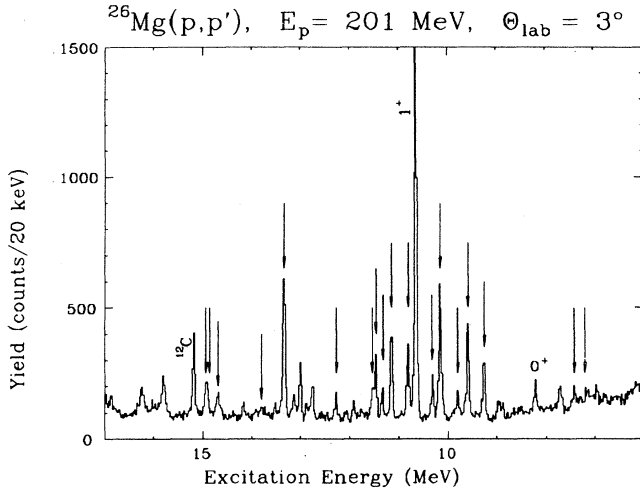


FIG. 5. Inelastic  $(p,p')$  spectrum measured at  $3^\circ$  on  $^{26}\text{Mg}$ .  $1^+$  states are labeled by arrows. The peak at 15.2 MeV is due to  $^{12}\text{C}$  contamination.

transitions, but with less confidence. Results from a  $(\gamma,\gamma')$  experiment,<sup>3</sup> where the range in excitation energies is limited by the neutron emission threshold at 11.1 MeV, together with earlier  $(e,e')$  data<sup>26</sup> are given for comparison. One should notice the large discrepancies in the  $B(M1)$  values measured by  $(e,e')$  and  $(\gamma,\gamma')$  experiments. We will compare our results to the  $B(M1)$  values reported in the much more recent  $(\gamma,\gamma')$  experiment,

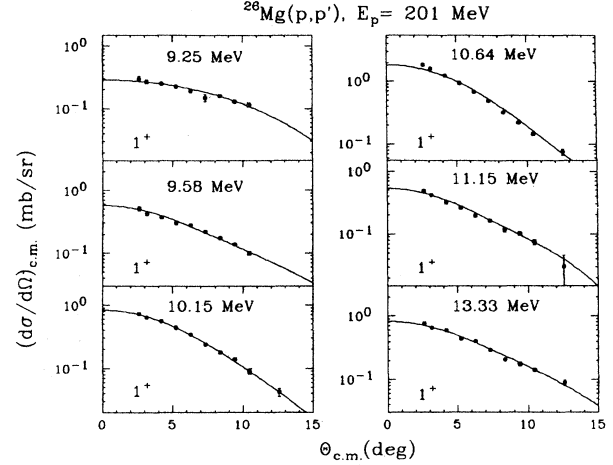


FIG. 6. Measured  $(p,p')$  angular distributions for some  $1^+$  states in  $^{26}\text{Mg}$  compared in shape with microscopic DWIA calculations.

where  $B(M1)$  values are obtained in a model-independent way.

Except for the  $1^+$  states reported at 8.23 MeV in the  $(\gamma,\gamma')$  reaction and at 8.52 MeV in the  $(e,e')$  reaction, which are not seen in the present experiment, there is good agreement with the excitation energies of the other  $1^+$  states reported in the electromagnetic reactions. The  $B(\sigma)$  values obtained in the present experiment are in

TABLE II. Excitation energies, cross sections at  $3^\circ$  and extracted  $B(\sigma)$  values obtained for  $1^+$  states in  $^{23}\text{Mg}$ . The results obtained in  $(e,e')$  and  $(\gamma,\gamma')$  experiments are given for comparison.

$E_x$ (MeV)	$(p,p')$ <sup>a</sup>		$(\gamma,\gamma')$ <sup>b</sup>		$(e,e')$ <sup>c</sup>	
	$(d\sigma/d\Omega)_{3^\circ}$ (mb/sr)	$B(\sigma)$ ( $\mu_n^2$ )	$E_x$ (MeV)	$B(M1)$ ( $\mu_n^2$ )	$E_x$ (MeV)	$B(M1)$ ( $\mu_n^2$ )
7.20	0.06±0.02	0.08±0.03				
7.42	0.09±0.02	0.14±0.06				
			8.23	0.11±0.02		
9.25	0.27±0.02	0.31±0.08	9.24	0.39±0.05	8.52	0.21±0.15
9.58	0.42±0.02	0.54±0.11	9.56	0.15±0.03	9.24	1.08±0.26
9.79	0.13±0.04	0.16±0.04			9.67	0.49±0.20
10.15	0.64±0.03	0.73±0.15	10.15	0.72±0.10	10.20	1.39±0.29
10.32	0.19±0.02	0.20±0.04	10.32	0.19±0.05		
10.64	1.59±0.04	2.32±0.56	10.65	1.35±0.15	10.65	1.95±0.40
10.81	0.30±0.02	0.45±0.10				
11.15	0.42±0.02	0.54±0.12			11.2	0.83±0.13
11.32	0.14±0.02	0.19±0.05				
11.46	0.26±0.02	0.32±0.07				
11.53	0.17±0.02	0.24±0.06				
12.26	0.11±0.02	0.21±0.05				
13.33	0.65±0.03	0.86±0.18			13.33	1.58±0.34
13.80	0.08±0.02	0.11±0.03				
14.69	0.10±0.02	0.13±0.04				
14.87	0.11±0.02	0.13±0.04				
14.93	0.14±0.02	0.20±0.05				

<sup>a</sup> Present work.

<sup>b</sup> Reference 3.

<sup>c</sup> Reference 26.

good agreement with the  $B(M1)$  values measured in the  $(\gamma, \gamma')$  experiment except for the states at 9.58 and 10.64 MeV. The ratios of  $B(\sigma)$  to  $B(M1)$  are, respectively,  $3.6 \pm 1.4$  and  $1.7 \pm 0.6$ . The discrepancy may be explained by a destructive interference between the orbital and spin terms in the electromagnetic excitation of these states. Such interference is predicted by the model only for a weak state located around 9 MeV (see Fig. 7); for all other states between 9 and 11 MeV the theory predicts a strong constructive interference between spin and orbital terms.

The theory<sup>5</sup> does not reproduce the detailed strength distribution as a function of excitation energy, but it does give a good agreement for the overall trend. The measured value for the centroid energy of the  $1^+$  strength, 11.08 MeV, is to be compared with the theoretical value of 11.38 MeV.

It is not possible in  $(p, p')$  to discriminate between  $1^+, T=1$  and  $1^+, T=2$  states in  $^{26}\text{Mg}$ . However, for the strong  $1^+$  state at 13.33 MeV we have made a tentative isospin assignment of  $T=2$  because the theory predicts a strong  $1^+, T=2$  state at 13.31 MeV (Fig. 7).

Charge exchange  $(p, n)$  results on  $^{26}\text{Mg}$  have been obtained at 135 MeV (Ref. 29) but a meaningful comparison with the present  $(p, p')$  results is very difficult because of the relatively poor energy resolution of the  $(p, n)$  experiment. In addition, the Gamow-Teller transitions observed in  $(p, n)$  lie on a relatively large continuum background and contain  $T_<$  components which are not present in the  $(p, p')$  reaction. Even a comparison of the relative strengths of a few discrete states near 10 MeV of excitation energy shows discrepancies. For example, the cross sections for the 10.64 and 10.32 MeV states in  $(p, p')$  are in the ratio of 8.4:1, whereas the analogs of these states seen in  $(p, n)$  at 10.8 and 10.5 MeV are in the ratio of 1.4:1.

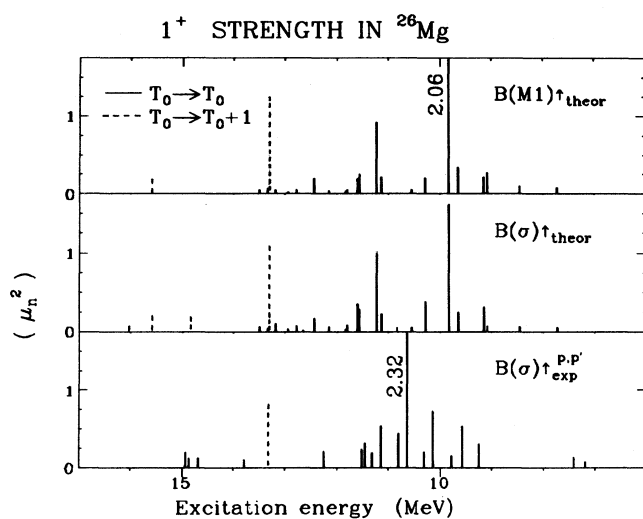


FIG. 7. Predicted spin-flip transition probabilities  $B(\sigma)$  and  $B(M1)$  values for  $1^+$  states in  $^{26}\text{Mg}$  compared with the  $B(\sigma)_{\text{exp}}^{p,p'}$  values extracted from the  $(p, p')$  cross sections. The dotted lines correspond to transitions to a final  $1^+$  state with isospin  $T=2$ . Strengths are given in  $\mu_n^2$ .

The total experimental  $(p, p')$  cross sections at  $3^\circ$  for all the  $1^+$  states listed in Table II, is  $5.9 \pm 0.4$  mb/sr. The theoretical  $(p, p')$  cross section at the same angle and for the same energy range is 7.98 mb/sr; the ratio of experimental to theoretical cross section is then  $R = 0.74 \pm 0.06$ . The uncertainty due to additional weakly excited  $1^+$  states is negligible compared to the uncertainty on the absolute cross section ( $\pm 5\%$ ).

For the  $(\gamma, \gamma')$  experiment, the total  $B(M1)$  value measured for all the states below 11.1 MeV is  $2.91 \pm 0.40 \mu_n^2$  to be compared to the total predicted strength (in the same range of excitation energy) of  $3.36 \mu_n^2$ . This gives a ratio of experimental to theoretical strength of  $0.87 \pm 0.12$ .

In the  $(p, n)$  experiment, only 57% of the total predicted Gamow-Teller strength is observed. This value is smaller than that determined for the  $1^+$  strength in the present  $(p, p')$  experiment. If some Gamow-Teller strength has been subtracted as part of the relatively large continuum background in  $(p, n)$ , this would help to explain the difference.

### C. $^{28}\text{Si}$

In Fig. 8 a spectrum is shown taken at a laboratory angle of  $3^\circ$ . Previous  $(p, p')$  results on  $^{28}\text{Si}$  are given in Ref. 10; however, the target used in that experiment was found later to be nonuniform. Therefore, new measurements were performed with different, uniform targets at TRIUMF and at the Orsay synchrocyclotron. The angular distribution for the strong  $1^+$  state at 11.45 MeV was carefully measured between  $2^\circ$  and  $12^\circ$ . The results are shown in Fig. 9 where we can see that there is an excellent agreement between the two measurements. The previous cross sections given in Ref. 10 have to be renormalized at each angle. The normalization factor varies smoothly from 2.2 to 2.9 between  $2^\circ$  and  $12^\circ$ .

The results from the present experiment are given in Table III and compared with results from  $(\gamma, \gamma')$  (Ref. 3) and  $(e, e')$ .<sup>30,31</sup> Compared to the table given in Ref. 10

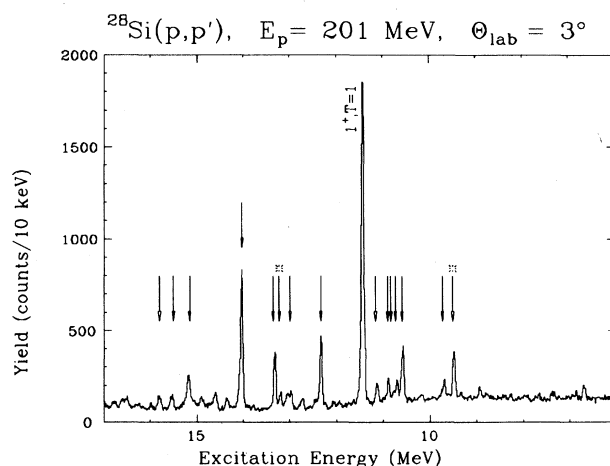


FIG. 8. Inelastic  $(p, p')$  spectrum measured at  $3^\circ$  on  $^{28}\text{Si}$ .  $1^+$  states are indicated by arrows. Isoscalar transitions are labeled by an asterisk.

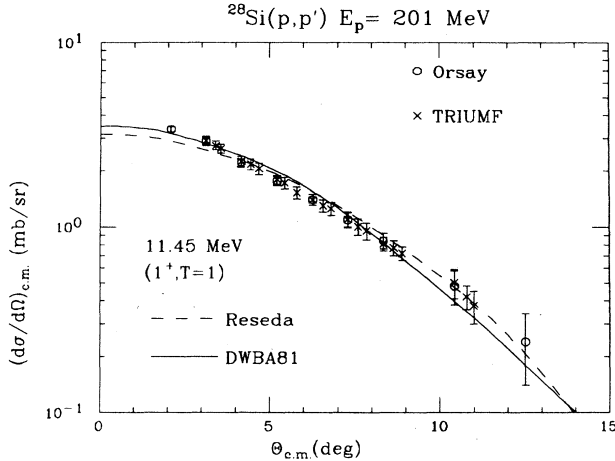


FIG. 9.  $(p,p')$  angular distributions measured at Orsay and TRIUMF for the strong  $1^+$  state at 11.45 MeV in  $^{28}\text{Si}$  are compared in shape with microscopic DWIA (code RESEDA) and DWBA calculations (code DWBA81).

there are some differences. The level at 8.33 MeV, which was listed as a  $1^+$ ,  $T=0$  state, is weakly excited, and its angular distribution is rather characteristic of a  $0^+$  state. A level at 13.22 MeV has a flat angular distribution similar to that of the state at 9.50 MeV and is therefore listed as a  $1^+$ ,  $T=0$  state. Five additional  $1^+$ ,  $T=1$  states are found at 9.72, 10.82, 11.16, 12.99, and 15.80 MeV.

The renormalized angular distributions have less steep slopes than those given in Ref. 10, thus improving the agreement with theory (see Fig. 9). However, for some states the theory still fails to reproduce the slope making

it difficult to extrapolate the measured angular distribution to zero degree. For these states the extracted  $B(\sigma)$  values have a large uncertainty. The predicted  $B(M1)$  and  $B(\sigma)$  values are compared to the extracted  $B(\sigma)$  values in Fig. 10. For the strongest  $T=1$  state, the predicted excitation energy (11.52 MeV) is in good agreement with the observed one (11.45 MeV); however, both the  $B(M1)$  and  $B(\sigma)$  values are underpredicted.

Experimentally,  $1^+$ ,  $T=0$  states are observed at 9.50 and 13.22 MeV which could correspond to the predicted states at 9.40 and 12.27 MeV. The ratio of their strengths is in agreement with the predicted ratio.

For most of the states, the predicted  $B(\sigma)$  values are larger than the predicted  $B(M1)$  values, implying destructive interference between the orbital and the spin terms in the electromagnetic excitation of these states. The magnitude of this interference varies from state to state. For the level predicted at 13.37 MeV, the  $B(\sigma)$  value is 40 times larger than the  $B(M1)$  value. This is in agreement with experiment in that a  $1^+$ ,  $T=1$  state observed at 13.35 MeV in  $(p,p')$  with a significant  $B(\sigma)$  value is not seen at all in the  $(e,e')$  reaction.

Constructive interference is only observed for the state at 10.90 MeV where the measured  $B(\sigma)$  value is less than half the measured  $B(M1)$  values. This is predicted by the model for a state at 11.19 MeV. The centroid energy value for the  $\Delta T=1$  states is 11.27 MeV, to be compared to the theoretical value of 12.78 MeV.

The ratio  $R_{\Delta T=0}$  of experimental to theoretical cross sections for the total isoscalar  $1^+$  strength is  $0.50 \pm 0.05$  in agreement with the results obtained at 200 MeV in Ref. 18. This value of  $R_{\Delta T=0}$  has been found to increase slightly with the proton bombarding energy between 200

TABLE III. Excitation energies, isospins, cross sections at  $3^\circ$ , and extracted  $B(\sigma)$  values obtained for  $1^+$  states in  $^{28}\text{Si}$ . The results obtained in  $(e,e')$  and  $(\gamma,\gamma')$  experiments are given for comparison.

$E_x$ (MeV)	$T$	$(p,p')$ <sup>a</sup>		$(\gamma,\gamma')$ <sup>b</sup>		$(e,e')$ <sup>c</sup>	
		$(d\sigma/d\Omega)_{3^\circ}$ (mb/sr)	$B(\sigma)$ ( $\mu_n^2$ )	$E_x$ (MeV)	$B(M1)$ ( $\mu_n^2$ )	$E_x$ (MeV)	$B(M1)$ ( $\mu_n^2$ )
9.50	0	0.49±0.04	0.09±0.01				
9.72	1	0.25±0.02	0.39±0.06				
10.59	1	0.56±0.06	0.83±0.12	10.60	0.28±0.11	10.59	0.19±0.04
10.73	1	0.21±0.02	0.32±0.04			10.72	0.15±0.03
10.82	1	0.13±0.02	0.21±0.04				
10.90	1	0.25±0.02	0.35±0.05	10.90	0.96±0.26	10.90	0.68±0.05
11.16	1	0.18±0.02	0.31±0.07				
11.45	1	2.90±0.10	3.32±0.24	11.45	4.01±0.50	11.44	4.07±0.22
12.33	1	0.65±0.05	0.73±0.14	12.33	0.84±0.23	12.33	0.81±0.06
12.99	1	0.15±0.01	0.23±0.05				
13.22	0	0.16±0.01	0.03±0.01				
13.35	1	0.46±0.04	0.81±0.14				
14.03	1	1.24±0.09	1.31±0.12			14.03	0.45±0.04
15.15	1	0.40±0.03	0.42±0.04			15.15	0.18±0.04
15.50	1	0.11±0.01	0.12±0.08			15.50	0.22±0.04
15.80	1	0.19±0.02	0.22±0.02				

<sup>a</sup> Present work.

<sup>b</sup> Reference 3.

<sup>c</sup> Reference 26.



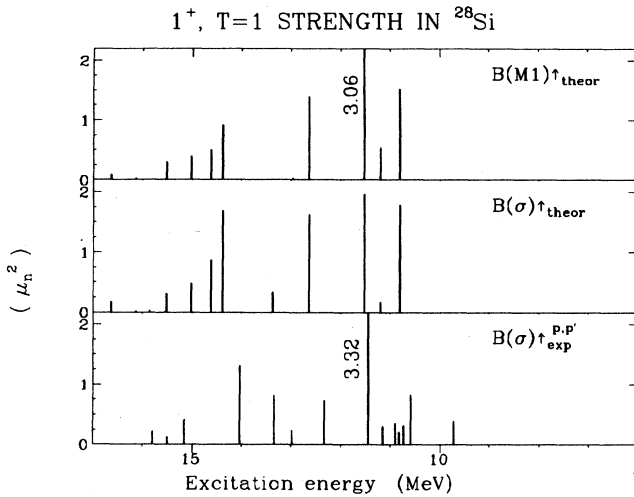


FIG. 10. Predicted spin-flip transition probabilities  $B(\sigma)$  and  $B(M1)$  values for  $1^+$  states in  $^{28}\text{Si}$  compared with the  $B(\sigma)_{\text{exp}}^{p,p'}$  values extracted from the  $(p,p')$  cross sections. Strengths are given in  $\mu_n^2$ .

and 250 MeV.<sup>18</sup> For the total isovector  $1^+$  strength, the ratio  $R_{\Delta T=1}$  is  $0.79 \pm 0.05$  in excellent agreement with the value of  $0.78 \pm 0.06$  measured in  $(e,e')$  scattering and also agrees with the value of  $0.89 \pm 0.09$  observed in the  $(\mathbf{p},\mathbf{p}')$  experiment of Ref. 18. It is interesting to notice that  $R_{\Delta T=0}$  is smaller than  $R_{\Delta T=1}$  suggesting that  $(\Delta-h)$  admixture is not the dominant quenching mechanism.

#### D. $^{32}\text{S}$

A spectrum from the  $^{32}\text{S}(p,p')$  reaction at a laboratory angle of  $3^\circ$  is shown in Fig. 11. A large number of possible  $1^+$  states is observed, most of which were not known previously. The spectrum is dominated at this angle by three strong  $1^+, T=1$  states at 8.13, 11.13, and 11.63 MeV excitation energy.

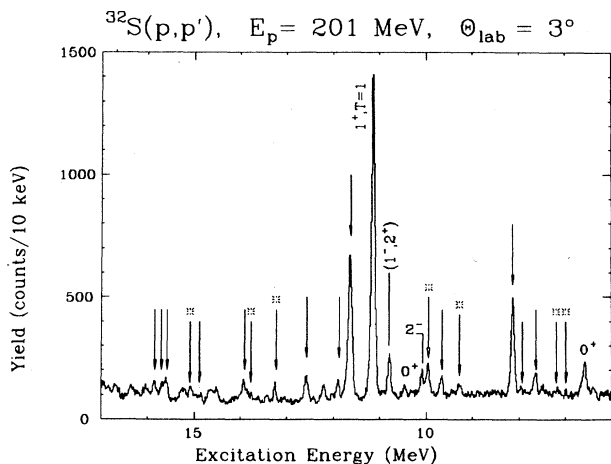


FIG. 11. Inelastic  $(p,p')$  spectrum measured at  $3^\circ$  on  $^{32}\text{S}$ .  $1^+$  states are indicated by arrows. Isoscalar transitions are labeled by an asterisk.

The angular distributions of these  $1^+$  states and a few other notable states are shown in Fig. 12 and compared in shape to theoretical predictions. The calculated angular distributions have a slightly flatter slope than the measured ones. This feature is common to all the  $1^+, T=1$  states in  $^{32}\text{S}$ . A similar situation exists in  $^{28}\text{Si}$ , whereas in the lighter  $s-d$  shell targets including  $^{24}\text{Mg}$ , the calculations matched the measured angular distributions very well.

There are several states observed in the spectrum at  $3^\circ$  which do not appear to be  $1^+$  states. Two of these states, at 6.58 and 10.43 MeV, have angular distributions characteristic of a transition to a  $0^+, T=0$  state. The state at 10.08 MeV is known<sup>25</sup> to be a  $2^-, T=1$  state and has indeed an angular distribution characteristic of an  $l=1$  transfer. Another state, at 10.80 MeV, has a rather flat angular distribution which peaks beyond  $10^\circ$  and is probably a state with  $J \geq 2$ . Since there is a known  $2^+$  state at 10.78 MeV and a  $J=1$  state at 10.786 MeV, the state observed at 10.80 MeV in the present experiment could be a mixture of  $2^+$  and  $1^-$  states.

In Table IV the excitation energies of all the  $1^+$  states observed in the present experiment are given together with measured cross sections at  $3^\circ$  and extracted  $B(\sigma)$  values; they are compared with results from  $(\gamma,\gamma')$ ,<sup>3</sup>  $(e,e')$  (Ref. 32) and recent  $(p,n)$  (Ref. 33) experiments. The predicted transition probabilities  $B(M1)$  and  $B(\sigma)$  values are compared to the extracted  $B(\sigma)$  values in Fig. 13 for all the  $1^+, T=1$  states.

Isoscalar  $1^+$  states will be discussed first. The main  $T=0$  state, which is predicted at 9.44 MeV, is observed at 9.93 MeV in the present experiment.

In the  $(p,n)$  reaction, a weak  $1^+, T=1$  state is reported at 7 MeV, which is not seen in the electromagnetic measurements. In the present  $(p,p')$  experiment a level at 6.98 MeV is weakly excited; its angular distribution is more consistent with a  $1^+, T=0$  assignment. The theory also predicts a  $1^+, T=0$  state at 7.125 MeV with a  $B(\sigma)$  value of  $0.025\mu_n^2$ , which agrees with our data.

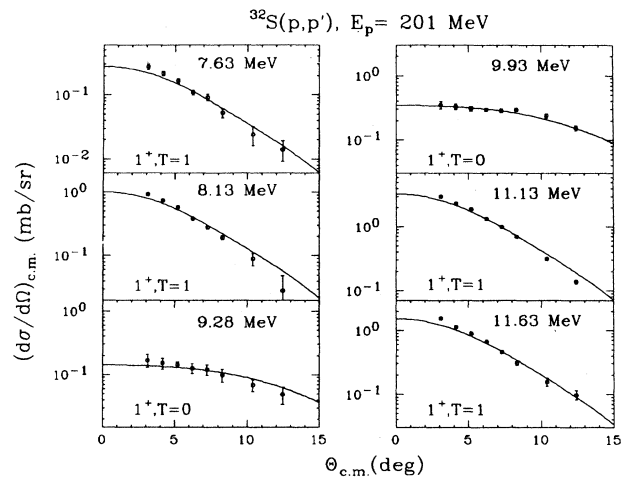


FIG. 12. Measured  $(p,p')$  angular distributions for some  $1^+$  states in  $^{32}\text{S}$  compared in shape with microscopic DWIA calculations.

The state at 7.19 MeV is known to be a  $1^+$  state,<sup>25</sup> but the isospin is uncertain. This state is only weakly excited and has a slope consistent with a  $1^+, T=0$  prediction; therefore an isospin  $T=0$  has been tentatively assigned. The states at 9.28 and 9.93 MeV are known to be  $1^+, T=0$  (Ref. 25) and have indeed flat  $(p, p')$  angular distributions. In the present experiment three additional  $1^+, T=0$  states are proposed at 13.23, 13.77, and with less confidence at 15.04 MeV.

Only the states to which an isospin  $T=0$  could be assigned without ambiguity were compared with the theoretical predictions of the total  $T=0$  strength. The centroid energy of the measured isoscalar  $1^+$  strength is 9.06 MeV, in good agreement with the theoretical value of 9.36 MeV. The ratio of experimental to theoretical isoscalar  $1^+$  strength is  $R_{\Delta T=0}=0.78\pm 0.14$ . The  $1^+, T=1$  states will be discussed now and compared with other experimental data.

There are two recent studies of  $^{32}\text{S}$  using inelastic elec-

tron scattering and nuclear resonance fluorescence. As mentioned earlier, this latter reaction can only study states below the particle emission threshold. The results from these experiments are also listed in Table IV. For the state at 8.13 MeV, both electromagnetic experiments give consistent  $B(M1)$  values which are also consistent, within the error bars, with the  $B(\sigma)$  value obtained in the present  $(p, p')$  experiment. The measured  $B(\sigma)$  and  $B(M1)$  values agree with those predicted for a state at 8.10 MeV which appears to be nearly a pure spin-flip state.

The  $(\gamma, \gamma')$  experiment also quotes a weak  $1^+$  state at 9.21 MeV which is not seen in either the  $(e, e')$  or  $(p, p')$  experiments. Both of the electromagnetic measurements find a  $1^+$  state near 9.66 MeV in  $^{32}\text{S}$ . This state is also observed in  $(p, p')$ . The extracted  $B(\sigma)$  values in  $(p, p')$  and  $(p, n)$  agree, but they are at least a factor of 2 smaller than the measured  $B(M1)$  values. This indicates an important orbital effect which is partly predicted by the

TABLE IV. Excitation energies, isospins, cross sections at  $3^\circ$ , and extracted  $B(\sigma)$  values obtained for  $1^+$  states in  $^{32}\text{S}$ . The results obtained in  $(e, e')$ ,  $(\gamma, \gamma')$ , and  $(p, n)$  experiments are given for comparison. For the  $(p, n)$  results a relative uncertainty of 15% is given for the total  $1^+$  strength; see Ref. 33 for more details. The  $(p, n)$  energies correspond to excitations energies in  $^{32}\text{S}$ .

$E_x$ (MeV)	$T$	$(p, p')$ <sup>a</sup>		$(\gamma, \gamma')$ <sup>b</sup>		$(e, e')$ <sup>c</sup>		$(p, n)$ <sup>d</sup>	
		$(d\sigma/d\Omega)_3$ (mb/sr)	$B(\sigma)$ ( $\mu_n^2$ )	$E_x$ (MeV)	$B(M1)$ ( $\mu_n^2$ )	$E_x$ (MeV)	$B(M1)$ ( $\mu_n^2$ )	$E_x$ (MeV)	$B(\sigma)$ ( $\mu_n^2$ )
6.98	0	0.10±0.02	0.02±0.01					7.00	0.04
7.19	(0)	0.07±0.02	0.02±0.01						
7.63	1	0.28±0.03	0.42±0.07						
7.92	1	0.09±0.02	0.10±0.02						
8.13	1	0.92±0.05	1.46±0.19	8.13	1.25±0.14	8.11	1.14±0.18	8.15	0.91
				9.21	0.12±0.04				
9.28	0	0.17±0.04	0.05±0.01						
9.66	1	0.13±0.02	0.17±0.02	9.66	0.43±0.11	9.68	0.69±0.18	9.79	0.19
9.93	0	0.35±0.04	0.10±0.02			(10.05)	0.57±0.22		
								10.73	0.07
11.13	1	2.96±0.10	4.08±0.53			11.12	2.40±0.22	11.06	2.66
11.63	1	1.56±0.10	2.38±0.35			11.63	1.26±0.20	11.58	0.82
11.88	1	0.23±0.03	0.37±0.06						
12.56	1	0.23±0.03	0.33±0.06					12.41	0.23
								13.06	0.09
13.23	(0)	0.13±0.03	0.04±0.01						
								13.29	0.06
								13.65	0.18
13.77	(0)	0.12±0.03	0.03±0.01						
13.90	1	0.18±0.03	0.24±0.03						
								14.36	0.15
								14.72	0.14
14.88	(1)	0.15±0.04	0.20±0.04						
15.04	(0)	0.20±0.03	0.04±0.01						
								15.30	0.08
15.58	1	0.23±0.03	0.28±0.05					15.60	0.08
15.70	1	0.12±0.03	0.16±0.04						
15.84	1	0.19±0.03	0.26±0.06						

<sup>a</sup> Present work.

<sup>b</sup> Reference 3.

<sup>c</sup> Reference 26.

<sup>d</sup> Reference 33.

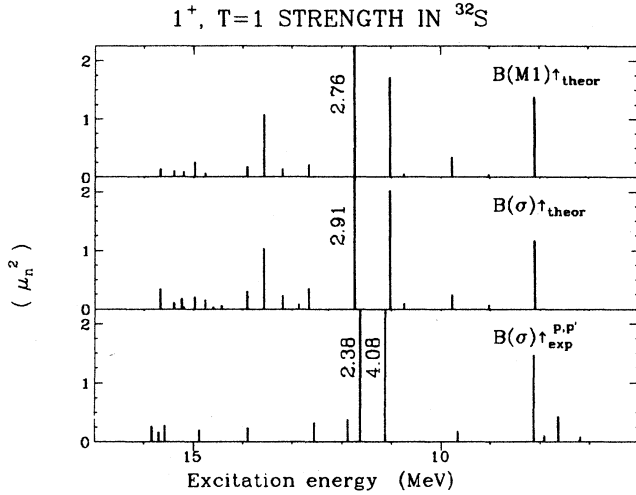


FIG. 13. Predicted spin-flip transition probabilities  $B(\sigma)$  and  $B(M1)$  values for  $1^+$  states in  $^{32}\text{S}$  compared with the  $B(\sigma)_{\text{exp}}^{p,p'}$  values excited from the  $(p,p')$  cross sections. Strengths are given in  $\mu_n^2$ .

model for a state at 9.77 MeV.

The  $(e,e')$  experiment tentatively assigns the spin parity of a state at 10.05 MeV to be  $1^+$ . No corresponding  $1^+$  state is seen near this energy in the  $(p,p')$  reaction. The other two strong  $1^+, T=1$  states seen in  $(p,p')$  are also observed in  $(e,e')$ , at 11.12 and 11.63 MeV. Two strong states are predicted theoretically at 11.03 and 11.74 MeV (Fig. 13), but the relative predicted strength does not agree with the experimental results. The  $B(\sigma)$  values obtained in the present  $(p,p')$  experiment are almost twice as large as the measured  $B(M1)$  values in the  $(e,e')$  experiment. Such a reduction of the  $B(M1)$  values compared to the  $B(\sigma)$  values is not predicted by the model.

Comparison with the  $(p,n)$  results obtained at 135 MeV incident proton energy<sup>33</sup> on a state by state basis is a little difficult for reasons similar to those given in the  $^{26}\text{Mg}$  discussion; namely, the energy resolution is about 270 keV, nearly three times poorer than in the present  $(p,p')$  experiment and many of the states of interest are only weakly excited and lie on a substantial continuum background. However, it is possible to make comparisons with the three most strongly excited analog states at 1.15, 4.06, and 4.58 MeV excitation energy corresponding to parent states in  $^{32}\text{S}$  at 8.15, 11.06, and 11.58 MeV (see Table IV). These three states contain about 75% of the total observed  $1^+, T=1$  strength in both the  $(p,p')$  and  $(p,n)$  experiments. There is also one other reasonably strong state seen in  $(p,p')$  at 7.63 MeV with an angular distribution clearly characteristic of a  $1^+, T=1$  state, the analog of which is not observed in  $(p,n)$ . The relative strengths of the three strongest states in  $^{32}\text{S}$  at 8.13, 11.13, and 11.63 MeV are in the ratio of 0.36:1.00:0.58 in  $(p,p')$ , while in  $(p,n)$  the same ratio for the analogs of these states is 0.34:1.00:0.31. Thus, even the relative strengths do not agree for all cases. This is difficult to understand if the excitation of  $1^+, T=1$  states in  $(p,p')$  and  $(p,n)$  reactions is dominated by the same piece of the

effective operator. It should be noted that in general the  $B(\sigma)$  values extracted from the  $(p,n)$  data<sup>33</sup> are smaller than those from the present data.

There are seven additional  $1^+, T=1$  states observed between 11.5 and 16.0 MeV. Since most of them are only weakly excited, a meaningful comparison with the  $(p,n)$  results is not possible.

In making comparisons between predicted and observed strengths, we shall again consider the summed strength rather than try to compare individual states. The centroid energy for all the  $1^+, T=1$  states listed in Table IV is 11.21 MeV to be compared with the predicted value of 11.86 MeV. The ratio of experimental to predicted  $1^+, T=1$  strength is  $R_{\Delta T=1} = 1.06 \pm 0.14$ . The large uncertainty in this ratio comes from the uncertainty in the absolute cross sections, plus the ambiguity in the  $1^+$  assignments to some of the high-lying states.

The quenching measured in the  $(p,n)$  experiment is  $R = 0.60 \pm 0.09$ , whereas our  $(p,p')$  experiment is consistent with there being no quenching. Some Gamow-Teller strength could be present in the continuum background subtracted in the  $(p,n)$  experiment, but the authors of Ref. 33 claim that there could be at most 20% of the observed strength present in the subtracted background. This still leaves a significant discrepancy with the ratio of experiment to theory between  $(p,p')$  and  $(p,n)$  which is not understood at present.

## V. SUMMARY AND CONCLUSIONS

The results presented in the present paper together with the published measurements on  $^{18}\text{O}$  (Ref. 8),  $^{20}\text{Ne}$ , and  $^{22}\text{Ne}$  (Ref. 9) allow some general conclusions about spin-flip excitations across a range of  $s$ - $d$  shell nuclei observed with the  $(p,p')$  reaction. The measured angular distributions clearly identify  $l=0$  angular momentum transfer and, with somewhat less certainty, allow one to distinguish  $0^+, 1^+, T=0$ , and  $1^+, T=1$  states. A number of previously unknown  $0^+$  and  $1^+$  states have been established.

The  $(p,p')$  results are compared with extensive shell-model predictions. For all the nuclei studied, except  $^{26}\text{Mg}$ , the excitation energy of the main  $1^+$  state is correctly predicted. The calculations indicate a significant orbital contribution which can interfere constructively or destructively with the spin contribution in the electromagnetic excitation of  $1^+$  states. For the main  $1^+$  state, the interference between orbital and spin terms is generally predicted to be constructive. A general feature of the predictions is that the interference is constructive for states located at excitation energies lower than that of the main  $1^+$  state and destructive for all the others. The comparison of the  $B(\sigma)$  values obtained from  $(p,p')$  cross sections with the  $B(M1)$  values measured in the electromagnetic reactions has been done to test these predictions. The model fails in reproducing in detail the magnitude of the orbital contribution; however, the general trend is correctly predicted.

In  $^{24}\text{Mg}$ , the level located at 9.83 MeV has a  $(p,p')$  angular distribution characteristic of a  $1^+, \Delta T=0$  transition; however, the fact that this state is also seen in

TABLE V. Ratios of experimental to theoretical  $1^+$  strengths in different  $s$ - $d$  shell nuclei:  $R_{\Delta T=0}$  (for the total isoscalar strength) and  $R_{\Delta T=1}$  (for the total isovector strength) are given for nuclei where isoscalar and isovector strengths can be separated.  $R_{\text{Total}}$  is for the total  $1^+$  strength. For  $^{18}\text{O}$  a range of  $R$  values is given, see Ref. 8 for more details. Systematic errors are included.

Nucleus	$^{18}\text{O}^a$	$^{20}\text{Ne}^b$	$^{22}\text{Ne}^b$	$^{24}\text{Mg}^c$	$^{26}\text{Mg}$	$^{28}\text{Si}$	$^{32}\text{S}$
$R_{\Delta T=0}$						$0.50 \pm 0.10$	$0.78 \pm 0.17$
$R_{\Delta T=1}$						$0.79 \pm 0.10$	$1.06 \pm 0.17$
$R_{\text{Total}}$	0.65–1.35	$1.00 \pm 0.10$	$0.73 \pm 0.07$	$1.13 \pm 0.11$	$0.74 \pm 0.11$	$0.74 \pm 0.10$	$1.04 \pm 0.17$

<sup>a</sup> Reference 8.

<sup>b</sup> Reference 9.

<sup>c</sup>  $R$  is given for model II.

( $\gamma, \gamma'$ ) (Ref. 3) and ( $e, e'$ ) (Ref. 26) experiments implies that it is not a pure  $T=0$  state. This is predicted by shell-model calculations allowing isospin mixing. The isoscalar and isovector  $1^+$  strengths could be studied separately only in  $^{28}\text{Si}$  and  $^{32}\text{S}$ .

The ratios of measured to predicted  $1^+$  strengths in  $^{24,26}\text{Mg}$ ,  $^{28}\text{Si}$ , and  $^{32}\text{S}$  are summarized in Table V. The results obtained previously for  $^{18}\text{O}$ ,  $^{20}\text{Ne}$ , and  $^{22}\text{Ne}$  are also given for comparison. While there are fairly large uncertainties in these values, especially for the  $T=0$  states, the trend is quite clear. There is no tendency for  $T=0$  states to be less quenched than  $T=1$  states. In fact, if anything, our results indicate the opposite trend in that the ratios of experimental to theoretical cross sections are generally smaller for the  $T=0$  states, corresponding to more quenching. Even though in  $^{28}\text{Si}$  this ratio has been found to increase slightly with the proton bombarding energy,<sup>18</sup> it is always smaller than for  $T=1$  states. This implies that the  $\Delta$ -hole explanation for quenching, which can only apply to the  $T=1$  states, is not the most important mechanism, at least in this mass region.

For the  $T=1$  states, the overall quenching observed in the ( $e, e'$ ) and ( $p, p'$ ) measurements is in agreement. Brown and Wildenthal<sup>5</sup> have predicted that the  $M1$  strength should be quenched somewhat less than the Gamow-Teller strength by an amount which varies from 14% in  $^{28}\text{Si}$  to 28% in  $^{24}\text{Mg}$ . Even taking into account the uncertainties on the  $R$  values, these predictions do not agree qualitatively with our observations. However, the small differences in quenching actually observed are in agreement with the calculations of Towner<sup>34</sup> which show that these differences, mainly arising from meson exchange current (MEC) corrections to the  $M1$  operator, are small. We note, however, that the MEC contribution calculated by Towner is much smaller than the empirical value obtained by Brown and Wildenthal (see Sec. 6.4 of

Ref. 34). (Note also that the conclusions of Ref. 5 are based mainly on a systematic study of low-lying  $M1$  transitions which have a significant orbital component.)

We must stress that there is a difference between ( $p, p'$ ) and ( $p, n$ ) quenching for the  $1^+, T=1$  strength using the same wave functions.<sup>5</sup> The  $R$  value of about 0.6 observed in ( $p, n$ ) agrees with the values of 0.54–0.58 predicted for Gamow-Teller transitions by Brown and Wildenthal.<sup>5</sup> Given that the ( $p, p'$ ) cross sections are dominated by the same type of isovector interaction as ( $p, n$ ) cross sections, it is surprising that we do not find similar quenching values. One might expect more strength to be found in ( $p, p'$ ) on the basis of the higher resolution, and hence better separation of peak and background relative to ( $p, n$ ). However, discrepancies appear in a level by level comparison as well as in the total strength. More theoretical and experimental work needs to be done to understand the origin of these discrepancies.

Perhaps the most striking feature of the results is the fact that if we consider the total summed strength for  $T=0$  and  $T=1$  states together, there is almost no quenching observed within the uncertainties. This agrees with the observation in  $^{12}\text{C}$  but contrasts with the situation in  $^{48}\text{Ca}$  and heavier nuclei. Perhaps this is because in heavier nuclei rather simpler wave functions are used in contrast with the wave functions used in the present analysis.

#### ACKNOWLEDGMENTS

The authors would like to thank O. Häusser and R. Sawafta for assistance in carrying out the absolute cross section measurements at TRIUMF, and U. E. P. Berg for lending his  $^{26}\text{Mg}$  target. This work was supported in part by the U.S. National Science Foundation under Grants INT-82-63242, PHY-86-11210, and PHY-87-14432.

<sup>1</sup>C. D. Goodman, *Spin Excitations in Nuclei* (Plenum, New York, 1984).

<sup>2</sup>A. Richter, Nucl. Phys. **A374**, 177c (1983); Phys. Scr. **T5**, 63 (1983).

<sup>3</sup>U. E. P. Berg, K. Ackermann, K. Bangert, C. Bläsing, W. Naatz, R. Stock, and K. Wienhard, Phys. Lett. **140B**, 191 (1984).

<sup>4</sup>N. Marty, *Weak and Electromagnetic Interactions in Nuclei*, edited by H. V. Klapdor (Springer-Verlag, Berlin, 1986), p. 268.

<sup>5</sup>B. A. Brown, Nucl. Phys. **A464**, 315 (1987); B. A. Brown and B. H. Wildenthal, *ibid.* **A474**, 290 (1987).

<sup>6</sup>M. Hino, K. Muto, and T. Oda, J. Phys. G **13**, 1119 (1987).

<sup>7</sup>W. E. Ormand and B. A. Brown (unpublished).

- <sup>8</sup>C. Djalali, G. M. Crawley, B. A. Brown, V. Rotberg, G. Caskey, A. Galonsky, N. Marty, M. Morlet, and A. Willis, *Phys. Rev. C* **35**, 1201 (1987).
- <sup>9</sup>A. Willis, M. Morlet, N. Marty, C. Djalali, G. M. Crawley, A. Galonsky, V. Rotberg, and B. A. Brown, *Nucl. Phys.* **A464**, 315 (1987).
- <sup>10</sup>N. Anantaraman, B. A. Brown, G. M. Crawley, A. Galonsky, B. H. Wildenthal, C. Djalali, N. Marty, M. Morlet, A. Willis, and J. C. Jourdain, *Phys. Rev. Lett.* **31**, 1409 (1984).
- <sup>11</sup>C. Djalali, Ph.D. thesis, University of Paris, Orsay, 1984.
- <sup>12</sup>B. H. Wildenthal, in *Progress in Particle and Nuclear Physics*, edited by D. H. Wilkinson (Pergamon, Oxford, 1984), Vol. 11, p. 5.
- <sup>13</sup>J. B. McGrory, *Phys. Lett.* **33B**, 327 (1970).
- <sup>14</sup>J. Comfort, program DW81 (unpublished).
- <sup>15</sup>R. Shaeffer and J. Raynal, program DWBA70 (unpublished).
- <sup>16</sup>M. A. Franey and W. G. Love, *Phys. Rev. C* **31**, 488 (1985).
- <sup>17</sup>P. Schwandt, H. O. Meyer, W. W. Jacobs, A. D. Bacher, S. E. Vigdor, M. D. Kaitchuck, and T. R. Donoghue, *Phys. Rev. C* **26**, 55 (1982).
- <sup>18</sup>O. Häusser, R. Sawafta, R. G. Jeppesen, R. Abegg, W. P. Alford, R. L. Helmer, R. Henderson, K. Hicks, K. P. Jackson, J. Lisantti, C. A. Miller, M. C. Vetterli, and S. Yen, *Phys. Rev. C* **37**, 1119 (1988).
- <sup>19</sup>R. Sawafta, Ph.D. thesis, University of Alberta, Alberta, 1987.
- <sup>20</sup>A. Willis, Ph.D. thesis, University of Paris, Orsay, 1968.
- <sup>21</sup>M. Lacombe, B. Loiseau, J. M. Richard, R. Vinh Mau, J. Côté, P. Pirès, and R. de Tourreil, *Phys. Rev. C* **21**, 861 (1980).
- <sup>22</sup>P. D. Kunz, program DWUCK, University of Colorado (unpublished).
- <sup>23</sup>G. R. Satchler, *Direct Nuclear Reactions* (Oxford University Press, London, 1983).
- <sup>24</sup>C. Djalali, N. Marty, M. Morlet, A. Willis, J. C. Jourdain, D. Böhle, U. Hartmann, G. Kuchler, C. Caskey, G. M. Crawley, and A. Galonsky, *Phys. Lett.* **164B**, 269 (1985).
- <sup>25</sup>P. M. Endt and C. Van der Leun, *Nucl. Phys.* **A310**, 1 (1978).
- <sup>26</sup>L. W. Fagg, *Rev. Mod. Phys.* **47**, 683 (1975).
- <sup>27</sup>B. D. Anderson, R. J. McCarthy, M. Ahmad, A. Fazely, A. M. Kalenda, J. N. Knudson, J. W. Watson, R. Madey, and C. C. Foster, *Phys. Rev. C* **26**, 8 (1982).
- <sup>28</sup>R. Sawafta, O. Häusser, R. Abegg, W. P. Alford, R. Henderson, K. Hicks, K. P. Jackson, J. Lisantti, C. A. Miller, M. C. Vetterli, and S. Yen, *Phys. Lett. B* **201**, 219 (1988).
- <sup>29</sup>R. Madey, B. S. Flanders, B. D. Anderson, A. R. Baldwin, C. Lebo, J. W. Watson, S. M. Austin, A. Galonsky, B. H. Wildenthal, C. C. Foster, *Phys. Rev. C* **35**, 2011 (1987); **36**, 1647 (1987).
- <sup>30</sup>R. Schneider, A. Richter, A. Schwierczinski, E. Spämer, O. Titze, *Nucl. Phys.* **A323**, 13 (1979).
- <sup>31</sup>A. Richter, *Nuclear Structure*, edited by K. Abrahams, K. Allaart, and A. E. L. Dieperink (Plenum, New York, 1981), p. 241.
- <sup>32</sup>P. E. Burt, L. W. Fagg, Hall Crannel, D. I. Sober, W. Stapor, J. T. O'Brien, J. W. Lightbody, X. K. Maruyama, R. A. Lindgren, and C. P. Sargent, *Phys. Rev. C* **29**, 713 (1984).
- <sup>33</sup>B. D. Anderson, T. C. Chitttrakarn, A. R. Baldwin, C. Lebo, R. Madey, P. C. Tandy, J. W. Watson, C. C. Foster, B. A. Brown, and B. H. Wildenthal, *Phys. Rev. C* **36**, 2195 (1987).
- <sup>34</sup>I. S. Towner, *Phys. Rep.* **155**, 264 (1987).